Mid-IR Photothermal Imaging with a Compact Ultrafast Fiber Probe Laser

Hui Liu[1,2], Atcha Totachawattana[1,2], Alket Mërtiri[3,2], Mi K. Hong[4], Tim Gardner[6], Shyamsunder Erramilli[2,4,5] and Michelle Y. Sander[1,2,3]

[1]Department of Electrical and Computer Engineering, Boston University, Boston, MA, United States
[2]BU Photonics Center, Boston University, Boston, MA, United States
[3]Division of Materials Science and Engineering, Boston University, Boston, MA, United States
[4]Physics Department, Boston University, Boston, MA, United States
[5]Department of Biomedical Engineering, Boston University, Boston, MA, United States
[6]Department of Biology, Boston University, Boston, MA, United States

ABSTRACT

A mid-IR photothermal imaging system is presented that features an integrated ultrafast erbium-doped fiber probe laser for the first time. With a mid-IR tunable quantum cascade laser (QCL) as the pump laser, vibrational molecular modes are excited and the thermally-induced changes in the refractive index are measured with a probe laser. The custom-built, all-fiber ultrafast probe laser at telecommunication wavelengths is compact, robust and thus an attractive source compared to bulky and alignment sensitive Ti:sapphire probe lasers. We present photothermal spectra and images with good contrast for a liquid crystal sample, demonstrating highly sensitive, label-free photothermal microscopy with a mode-locked fiber probe laser.

Keywords: Mid-IR Spectroscopy, Photothermal Imaging, Ultrafast Laser, Fiber Laser

1. INTRODUCTION

Photothermal spectroscopy[1,2] has emerged as a sensitive, label-free optical spectroscopy method. Photothermal spectroscopy relies on direct absorption of a pump laser light, which induces localized sample heating in a non-equilibrium state. Thermally induced changes in the index of refraction are then measured by a probe laser. As a nondestructive and contactless technique, changes in the physical and thermodynamic properties due to absorption of light are detected. In the visible regime, high signal to noise and high contrast photothermal spectroscopy and imaging have recently been demonstrated, down to the single molecule level[3–7].

With the development of high power tunable quantum cascade lasers (QCL)[8] that feature high spectral brightness, new applications and frontiers in mid-infrared (mid-IR) spectroscopy have emerged[9]. The mid-IR region is particularly interesting due to the large number of characteristic vibrational modes of molecules in this "fingerprint" region of the electromagnetic spectrum. Extension of photothermal spectroscopy to the mid-IR is very attractive as it can rely on the strong absorption in the mid-infrared for spectroscopic studies and imaging without the need of a perturbing label.

A probe laser at visible and near-infrared wavelengths has the advantage that it can be detected with commercially available, highly sensitive photodetectors and does not require complex, generally cryogenically cooled mid-IR detectors like in other infrared spectroscopic methods such as Fourier Transform Infrared Spectroscopy (FTIR). Recently, photothermal measurements with a mid-IR quantum cascade pump laser were demonstrated, using a Helium-Neon laser[10] or Ti:sapphire laser[11,12] as probe lasers. Erbium-doped fiber lasers can operate in a wavelength regime between

1530nm to 1625nm, where there is low absorption in many chemical and biological samples, which is critical to providing good measurement contrast. Thus, fiber lasers with high coherence and stability make an attractive probe laser source, as they feature a compact footprint, robust performance metrics and they are compatible with readily available commercial components at telecommunication wavelengths. In combination with the long-wavelength pump, the erbium-doped probe laser offers a system operating at eye-safe wavelengths.

Here, we report the first mid-IR photothermal spectroscopy system using a QCL as the pump laser and a compact ultrafast Er-doped fiber laser as the probe to study the characteristic band of a 6μm-thick liquid crystal layer of 4-Octyl-4'-Cyanobiphenyl (8CB). Linear and nonlinear photothermal studies of the 8CB liquid crystal were observed with high contrast using the all-fiber probe laser at telecommunication wavelengths. Ultrafast fiber lasers provide the potential for low phase noise, reduced detector shot noise at higher repetition rates[13] with low relative intensity noise in photothermal systems and they can generate different colors through nonlinear processes for different sample needs.

2. EXPERIMENTAL SETUP

2.1 Pump Laser: Quantum Cascade Laser

Our pump beam is a table-top mid-IR QCL from Daylight Solutions (Figure 1a) that operates around 6μm and can be tuned to molecular vibrational modes within the 1575cm^{-1} to 1740cm^{-1} wavenumber range of the laser. It provides compact and robust packaging with high brightness that can exceed that of synchrotron[14] and other large relativistic electron-accelerator-based sources. The QCL is operated in pulsed mode, with pulse durations around 500ns at a 100kHz repetition rate. Thus, lock-in detection technology can be used to reduce the background.
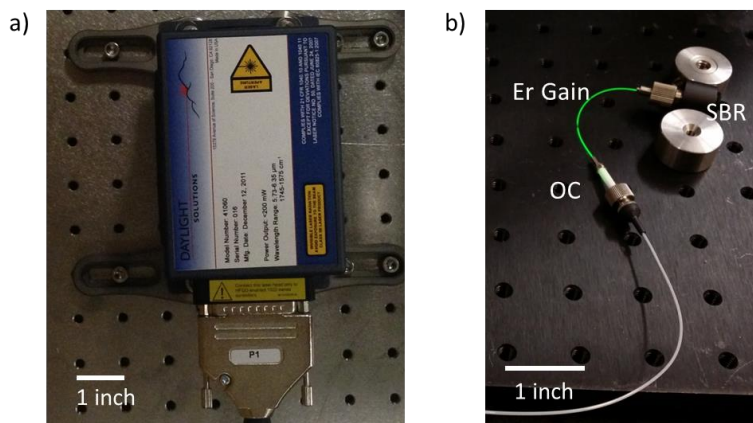

Figure 1. (a) Tunable, pulsed, mid-IR quantum cascade laser in the photothermal system. The pulse duration is 500ns with a 100kHz repetition rate. (b) Compact, ultrafast Er-doped fiber laser. The fiber laser cavity is 10cm long and the green fluorescence of the Erbium-doped gain fiber is clearly visible.

2.2 Probe Laser: Ultrafast Er-doped Fiber Laser

For a compact laser cavity, an ultrafast fiber laser based on soliton mode-locking in combination with a saturable Bragg reflector (SBR) is constructed[15–17]. While free-space focusing onto the SBR provides flexibility in repetition rate tuning[18], a SBR butt-coupled configuration features reduced intracavity coupling losses and can support short femtosecond pulses with higher energy. The self-starting laser is stable over long periods of time.

The schematic of the fiber laser is shown in Figure 2. A highly-doped, anomalously dispersive Er-doped gain fiber (Liekki Er80-8/125, with anomalous dispersion of -20fs^2/mm) was connected to a coated fiber ferrule which works as a 10% output coupler (OC) for the fiber laser while allowing high transmission of the pump light. When the gain fiber was directly butt-coupled to the SBR, intense thermal heating at the surface of the semiconductor saturable absorber could

cause damage to the fiber tip and saturable absorber[19]. Therefore, a short piece (~9mm) of passive single-mode fiber (SMF28e) was spliced to the other end of the gain fiber as a buffer to spatially separate the hot gain fiber core from the SBR. In addition, to reduce absorption of the pump light, a dielectric pump-reflective coating was deposited directly on the surface of the SBR.
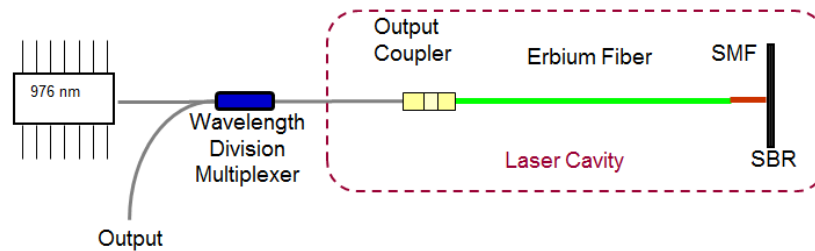

Figure 2. Schematic of the femtosecond all-fiber probe laser. The Er-doped gain fiber is butt-coupled to a 10% output coupler and spliced to a piece of single mode fiber butt-coupled to a saturable Bragg reflector for mode-locked operation.

The fiber laser showed stable long-term operation. In the following experiments, the Er-doped gain fiber was pumped with 387mW of pump power through the wavelength division multiplexer. With a 10% output coupling ratio, an output power of 11.5mW was obtained. The mode-locked spectrum is shown in Figure 3a with a full-width half maximum (FWHM) spectral bandwidth of 6.5nm centered around 1558.7nm. This spectral bandwidth corresponds to a calculated transform limited pulse duration of 392fs. Low phase noise and timing jitter values for the free-running laser were confirmed[19]. The repetition rate of this particular fiber geometry was 1.04GHz. The design can be modified to operate at lower repetition rates.
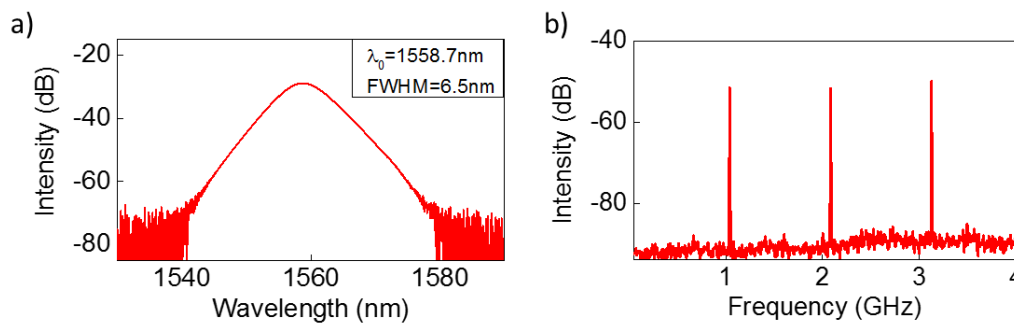

Figure 3. (a) Mode-locked spectrum of the fiber laser with center wavelength at 1558.7nm and bandwidth of 6.5nm. (b) RF spectrum of the fiber laser with repetition rate of 1.04GHz.

2.3 Photothermal Set-Up

The pump-probe set-up of our photothermal configuration utilizes a pump laser to excite the characteristic resonances. A probe laser at wavelengths far away from the vibrational bands of the sample serves to detect the thermally induced changes of the refractive index. Figure 4 shows the schematic of our mid-IR photothermal measurement system: The pump beam (QCL) and the Er-doped fiber laser probe beam (EDFL) are collinearly combined using a dichroic mirror and focused by a ZnSe objective onto the sample. The scattered signal is detected using an amplified InGaAs photodetector, connected to a low noise pre-amplifier and lock-in amplifier.

The mid-IR QCL can be tuned over a wavenumber range of $1575cm^{-1}$ to $1740cm^{-1}$, where detailed spectral studies of several vibrational bands can be conducted. A liquid crystal, 4-Octyl-4'-Cyanobiphenyl (8CB), was chosen as a representative study for molecules with strong absorption resonances. We chose a 6μm-thick liquid crystal 8CB layer embedded between two CaF_2 windows. Measurements were conducted at room temperature where the liquid crystal was in the smectic-A phase.
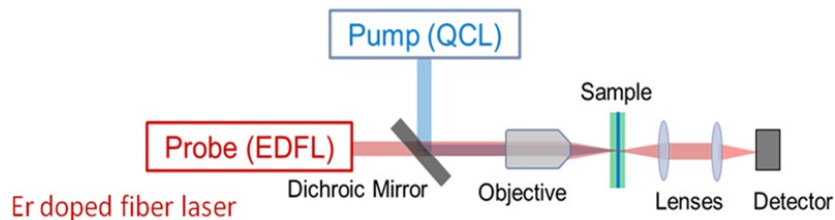
Figure 4. Schematic of mid-IR photothermal measurement set-up with QCL pump and Er doped fiber probe laser.

3. EXPERIMENTAL RESULTS

3.1 Linear Photothermal Spectrum

Photothermal measurements were conducted for varying QCL pump power values. At low pump powers, a linear signal response was measured and the photothermal measurements show good agreement with the FTIR spectrum. Figure 5a shows the photothermal spectrum of the 6μm-thick 8CB sample, characterizing the CH-scissoring mode centered at 1607cm^{-1} with a high spectral contrast ratio of 730. The spectrum is smoother and less noisy than previous measurements conducted with a Ti:sapphire laser[20]. Figure 5b presents the corresponding FTIR spectrum of the same sample. Both spectra can be fitted to a Gaussian curve, with the photothermal measurement featuring a slightly narrower full width half maximum (FWHM) of 4.3cm^{-1} compared to 4.6cm^{-1} for the FTIR.
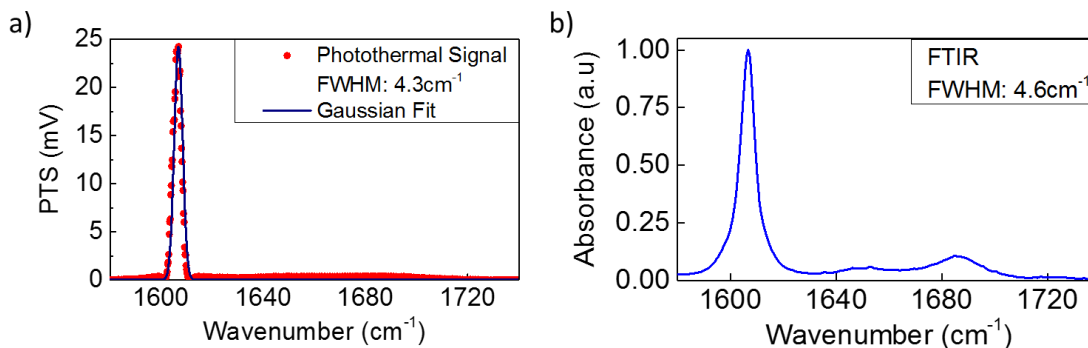

Figure 5. (a) Linear Photothermal spectrum of 6μm-thick 8CB sample. (b) FTIR spectrum of the same sample.

For a constant pump power, the probe power was varied and the photothermal spectral response recorded. As depicted in Figure 6, the photothermal signal scaled linearly with probe laser power, as previously also reported by Lu et al.[7]. The linear photothermal signal dependence on the probe power continued even when we amplified the laser output power with a custom-built erbium-doped fiber amplifier (EDFA) up to values of 74.5mW. This linear trend indicates that the fiber probe does not encounter any saturation or absorption effects for any of the operating powers. Figure 6 displays the average and standard deviation of three independent photothermal measurements for each probe power. The small standard deviation of the signal (the error bars are of the same scale as the symbol used for the measurement points) underlines the high reproducibility and good stability of our system.

By raster-scanning over a spatial selection of the sample, hyperspectral images were obtained on both liquid crystal samples and biological samples. High imaging contrast was achieved, especially with the pump wavelength tuned to the peak of the absorption resonances. In addition, the tuning range of our QCL laser overlapped with the amide-I absorption band resonance peak around 1660cm^{-1}. Studies of the amide-I absorption band can reveal conformational changes in protein, misfolding of the protein structure and associated lipids and thus relay valuable insights into tissue sections and neurological disorders. The photothermal measurements were extended to biological songbird brain sections where the amide-I band provided good imaging contrast, with the expectation to gain more detailed understanding of memory formation mechanisms.
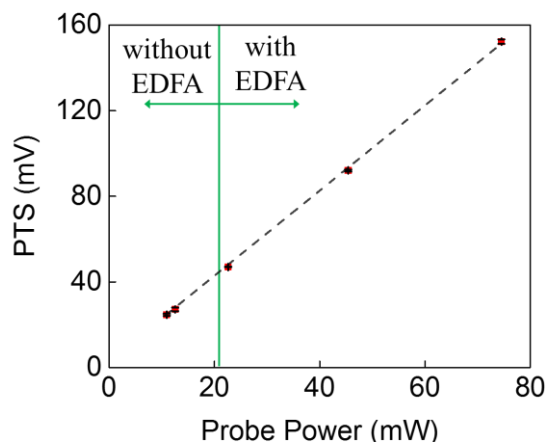
Figure 6. Photothermal signal dependence on fiber probe power. The average of three measurements for each probe power is plotted and the standard deviation is indicated by error bars (which are of the same scale as the symbols associated with each plotted point). The dotted line shows that the photothermal signal scales linearly with increasing probe power. The green line indicates which data points where taken with and without an erbium-doped fiber amplifier (EDFA).

3.2 Nonlinear Photothermal Spectrum

When increasing the QCL pump power but keeping the probe laser parameters constant, a nonlinear photothermal response was recorded starting for QCL pump currents around 500mA, as shown in Figure 7. Instead of a continuous monotonic increase of the photothermal spectral signature, a pitchfork bifurcation[12] characterized by a peak splitting process of the main resonance sets in. Peak splitting was first reported by Zharov[21] in the visible to near infrared and explained by the formation of "nano-bubbles" that reduce the magnitude of the photothermal signal collected. In the mid-infrared, nonlinear photothermal spectroscopy and pitchfork bifurcation was first demonstrated and analyzed by Mertiri et al[12]. We find that for our sample with increasing QCL pump powers, multiple peak splitting and peak narrowing is recorded. In addition, the weak signal in the linear regime between 1640cm^{-1} and 1700cm^{-1} is strongly enhanced. Thus, nonlinear photothermal spectroscopy offers the potential of higher spectral resolution and strong signal enhancements compared to the linear regime. More detailed studies of this phenomena are ongoing.
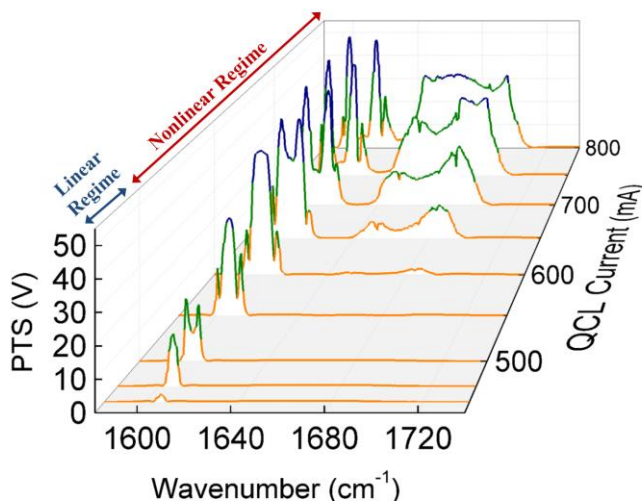

Figure 7. Nonlinear spectrum evolution of the liquid crystal sample depending on varying pump current. Pitchfork bifurcation, spectral narrowing and signal enhancement are recorded in the nonlinear regime.

4. CONCLUSION

In summary, we have demonstrated a compact mid-IR photothermal imaging system that incorporates an integrated ultrafast mode-locked fiber laser as a probe. Combined with a mid-IR QCL as the pump laser, the system was used to characterize the linear and nonlinear spectral behaviors of a 6μm-thick 8CB sample. The presented results demonstrate the potential for highly sensitive spectroscopy applications in an eye-safe wavelength regime. The attractive characteristics of ultrafast fiber lasers make them a strong candidate as a low noise and robust laser source with turn-key operation for spectroscopy.

REFERENCES

[1] Long, M. E., Swofford, R. L. & Albrecht, A. C. "Thermal lens technique: a new method of absorption spectroscopy" *Science* **191,** 183–185 (1976).

[2] Bialkowski, S. E. [Photothermal Spectroscopy Methods for Chemical Analysis*].* **134,** (John Wiley and Sons, 1996).

[3] Lasne, D. *et al.* "Label-free optical imaging of mitochondria in live cells" *Opt Express* **15,** 14184–14193 (2007).

[4] Cognet, L. *et al.* "Single metallic nanoparticle imaging for protein detection in cells" *Proc. Natl. Acad. Sci.* **100,** 11350–11355 (2003).

[5] Gaiduk, A., Yorulmaz, M., Ruijgrok, P. V. & Orrit, M. "Room-Temperature Detection of a Single Molecule's Absorption by Photothermal Contrast" *Science* **330,** 353–356 (2010).

[6] Gaiduk, A., Ruijgrok, P. V., Yorulmaz, M. & Orrit, M. "Detection limits in photothermal microscopy" *Chem. Sci.* **1,** 343–350 (2010).

[7] Lu, S., Min, W., Chong, S., Holtom, G. R. & Xie, X. S. "Label-free imaging of heme proteins with two-photon excited photothermal lens microscopy" *Appl. Phys. Lett.* **96,** 113701 (2010).

[8] Faist, J. *et al.* "Quantum Cascade Laser",*Science* **264,** 553–556 (1994).

[9] Capasso, F. *et al.* "New frontiers in quantum cascade lasers and applications" *IEEE J. Sel. Top. Quantum Electron.* **6,** 931–947 (2000).

[10] Farahi, R. H., Passian, A., Tetard, L. & Thundat, T. "Pump–probe photothermal spectroscopy using quantum cascade lasers" *J. Phys. Appl. Phys.* **45,** 125101 (2012).

[11] Mërtiri, A. *et al.* "Mid-infrared photothermal heterodyne spectroscopy in a liquid crystal using a quantum cascade laser" *Appl. Phys. Lett.* **101,** 044101 (2012).

[12] Mertiri, A. *et al.* "Nonlinear Midinfrared Photothermal Spectroscopy Using Zharov Splitting and Quantum Cascade Lasers" *ACS Photonics* **1,** 696–702 (2014).

[13] Quinlan, F. *et al.* "Exploiting shot noise correlations in the photodetection of ultrashort optical pulse trains" *Nat. Photonics* **7,** 290–293 (2013).

[14] Carr, G. L., Dumas, P., Hirschmug, C. J. & Williams, G. P. "Infrared synchrotron radiation programs at the National Synchrotron Light Source" *Il Nuovo Cimento D* **20,** 375–395 (1998).

[15] Haus, H. "Theory of mode locking with a slow saturable absorber" *IEEE J. Quantum Electron.* **QE-11,** 736 – 746 (1975).

[16] Paschotta, R. & Keller, U. "Passive mode locking with slow saturable absorbers" *Appl. Phys. B* **73,** 653–662 (2001).

[17] Kartner, F. X., Jung, I. D. & Keller, U. "Soliton mode-locking with saturable absorbers" *Sel. Top. Quantum Electron. IEEE J. Of* **2,** 540 –556 (1996).

[18] Sander, M. Y. *et al.* "1 GHz femtosecond erbium-doped fiber lasers" in *Lasers Electro-Opt. CLEO Quantum Electron. Laser Sci. Conf. QELS 2010 Conf. On* 1–2 (2010).

[19] Byun, H. *et al.* "Compact, stable 1 GHz femtosecond Er-doped fiber lasers" *Appl. Opt.* **49,** 5577–5582 (2010).

[20] Sander, M. Y., Liu, H., Mertiri, A., Totachawattana, A. & Erramilli, S. "Mid-IR Photothermal Spectroscopy with an Integrated Fiber Probe Laser" in *CLEO 2014* SM2E.3 (Optical Society of America, 2014). doi:10.1364/CLEO_SI.2014.SM2E.3

[21] Zharov, V. P. "Ultrasharp nonlinear photothermal and photoacoustic resonances and holes beyond the spectral limit" *Nat. Photonics* **5,** 110–116 (2011).